www.czasopisma.pan.pl PAN POLSKA AKADEMIA NAUK www.journals.pan.pl

A R C H I V E S O F M E T A L L U R G Y A N D M A T E R I A L S

Volume 59 2014 Issue 4

DOI: 10.2478/amm-2014-0214

A. CWUDZIŃSKI*

NUMERICAL PREDICTION OF HYDRODYNAMIC CONDITIONS IN ONE STRAND TUNDISH. INFLUENCE OF THERMAL CONDITIONS AND CASTING SPEED

NUMERYCZNA PROGNOZA WARUNKÓW HYDRODYNAMICZNYCH W JEDNOŻYŁOWEJ KADZI POŚREDNIEJ. WPŁYW WARUNKÓW CIEPLNYCH I PRĘDKOŚCI ODLEWANIA

This paper reports the results of computer simulations of the flow of liquid steel in a single-nozzle tundish, which describe the flow hydrodynamics, depending on the thermal conditions and casting speed. In this paper, five casting speeds, namely 0.3, 0.6, 0.9, 1.2 and 1.5 m/min., have been examined. In view of the fact that tundishes are being equipped with various flow control devices and the process of creating specific hydrodynamic conditions is influenced also by the temperature gradient, computer simulations of liquid steel flow under isothermal and non-isothermal conditions were performed. Computer simulations of liquid steel flow were performed using the commercial program Ansys-Fluent®. In order to explain the phenomena occurring in the tundish working space, the buoyancy number (Bu) has been calculated. The next research step in the analysis of the flow pattern forming in different casting conditions was to record the E and F-type RTD characteristics and to describe the pattern of flow.

Keywords: tundish, steel flow, numerical modeling, thermal conditions, casting speed

Praca przedstawia wyniki symulacji komputerowej opisującej wpływ warunków cieplnych i prędkości odlewania na przepływ ciekłej stali w jedno-wylewowej kadzi pośredniej. W pracy testowano pięć prędkości odlewania: 0,3; 0,6; 0,9; 1,2 i 1,5 m/min. Ze względu na gradient temperatury powstający w objętości ciekłej stali i stosowanie w kadziach pośrednich urządzeń sterujących przepływem, symulacje komputerową przepływu ciekłej stali wykonano dla warunków izotermicznych i nieizotermicznych. Symulacje komputerową przepływu ciekłej stali wykonano za pomocą programu Ansys-Fluent®. Dla wyjaśnienia zjawisk występujących w przestrzeni roboczej kadzi pośredniej obliczono liczbę wyporu (Bu). Do analizy struktury hydrodynamicznej przepływu ciekłej stali w różnych warunkach odlewania zarejestrowano krzywe czasu przebywania typu E i F.

1. Introduction

In the continuous steel casting process, the majority of steel semi-finished products are produced, which are intended for plastic working into tubes, plates or shapes. The components of a Continuous Steel Casting (CSC) machine include a steelmaking ladle, a tundish, a mould and a secondary cooling zone. Liquid steel flows into the mould via the tundish. In the mould solidifying steel shell is formed. Next in the secondary cooling zone cast strand is shaped. Therefore, the description of phenomena occurring in the tundish, mould and secondary cooling zone being an integral parts of the CSC machine is the key to the elimination of the factors adversely affecting the casting process. General knowledge about phenomenon of heat transfer between liquid steel – mould, liquid steel – mould powder, liquid steel – solidifying shell – spray cooling system and behaviour of mould powder on the liquid steel and solidifying shell surface is essential for correct work of continuous casting machine [1-6]. One of the tasks of the tundish is to maintain the constant hydrostatic pressure in the tundish, which assures the stable pouring of the mould. Another task is to protect the liquid steel through the use of insulating and refining powders and submerged entry nozzles. At the same time, by using flow control devices, the liquid flow hydrodynamics is influenced, which has an effect on the quality of the steel being cast [7-8]. The continuous steel casting process is a dynamic process which changes the physicochemical condition of the metal being cast. The fluctuation of temperature influences the viscosity and density of the liquid steel, and thus also its flow. The stream patterns occurring in the tundish working space in the turbulent motion system form hydrodynamic states which are characteristic of given tundish furniture [9-13]. In addition, a parameter varying during the course of the CSC process is the casting speed, which is dependent on the casting dimensions, steel grade and the metallurgical length of the plant, including the cooling system. Therefore, the casting speed will have an effect on the velocity of liquid steel flow and hydrodynamic structure in the tundish [14-15].

* CZESTOCHOWA UNIVERSITY OF TECHNOLOGY, DEPARTMENT OF METALS EXTRACTION AND RECIRCULATION, FACULTY OF MATERIALS PROCESSING TECHNOLOGY AND APPLIED PHYSICS, 19 ARMII KRAJOWEJ AVE, 42-200 CZĘSTOCHOWA, POLAND

For the analysis of the phenomena occurring in the tundish, mathematical models can be successfully used, which describe the mechanisms of mass, momentum and energy exchange in virtual systems reflecting the actual metallurgical plants. This paper reports the results of computer simulations of the flow of liquid steel in a single-nozzle tundish, which describe the flow hydrodynamics, depending on the thermal conditions and casting speed.

2. Characterization of the test facility

The facility under investigation is a single-nozzle tundish designed for casting concast slabs (Figs. 1a and 1b). The nominal capacity of the tundish is 30 Mg. Currently, the tundish is furnished with a low dam installed before the bottom step in the stopper rod system area. The height of the low dam is 0.12 m. The dam incorporates two 0.14×0.05 m overflow windows arranged symmetrically relative to the tundish axis. On the pouring zone side, the tundish is furnished with an overflow trough that protects the tundish against overfilling. The tundish shape resembles a wedge narrowing towards the pouring zone. The submerged entry nozzle discharge orifice and the ladle shroud pouring gate are located in the tundish axis at a distance of 2.915 m from each other. The inner diameters of the openings supplying liquid steel to the tundish and to the mould are identical, being equal to 0.07 m. Figure 1c presents a tundish with 0.3 m-high dam on a scale of 1:1. This dam has been positioned perpendicularly to the tundish axis between the side walls. Figure 1d presents a tundish virtual model with subflux turbulence controller (STC) on a scale of 1:1, which are intended for numerical simulation. The working space of STC has been made in the shape of a bowl. STC was installed in the axis of the liquid steel stream feeding the tundish. A tundish in the form of virtual models was prepared for numerical simulations using the Gambit 2.4 software program.

3. Testing methodology

The software program Ansys-Fluent® is the world's recognized CFD program that finds application in studies on the motion of steel in the steelmaking technology. The basic mathematical model equations describing the phenomena under examination are as follows:

$$\frac{\partial \rho}{\partial t} + \nabla (\rho u) = 0 \tag{1}$$

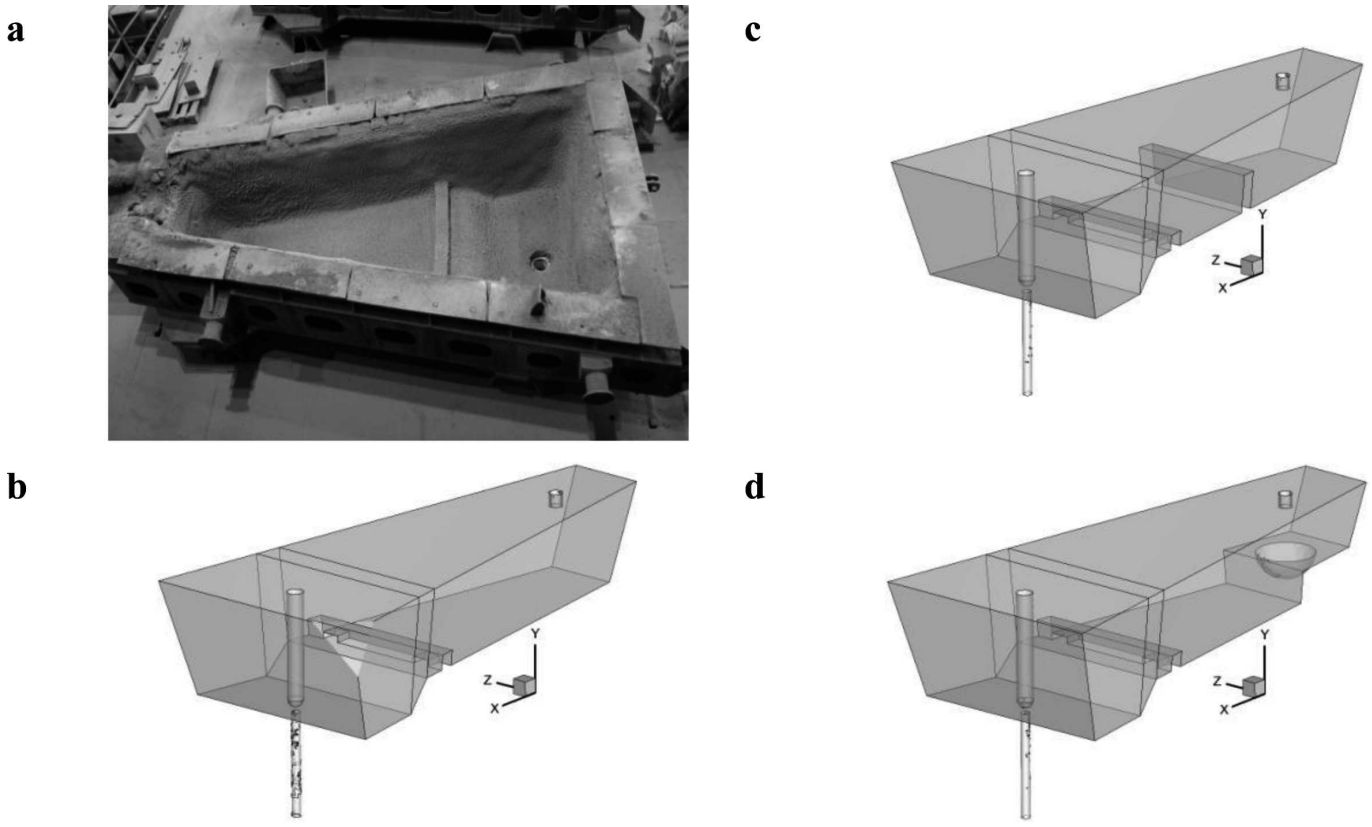

Fig. 1. Test facility: a) industrial tundish, b) virtual model of tundish with low dam, c) virtual model of tundish with high dam, d) virtual model of tundish with STC

$$\frac{\partial}{\partial t}(\rho u) + \nabla(\rho u u) = -\nabla p + \nabla(\bar{\bar{\tau}}) + \rho g \tag{2}$$

$$\bar{\bar{\tau}} = \mu\left[\left(\nabla u + \nabla u^T\right) - \frac{2}{3}\nabla u I\right] \tag{3}$$

$$\frac{\partial}{\partial t}(\rho E) + \nabla(u(\rho E + p)) = \nabla\left(k_{eff}\nabla T - \sum_j h_j J_j + (\bar{\bar{\tau}}_{eff} u)\right) \tag{4}$$

$$E = h - \frac{p}{\rho} + \frac{u^2}{2} \tag{5}$$

$$\rho = 8300 - 0.7105T \tag{6}$$

$$\frac{\partial C_i}{\partial t} + \nabla(-D_i \nabla C_i + C_i u) = 0 \tag{7}$$

where: C_i – concentration of the tracer (kg), $\bar{\bar{\tau}}$– stress tensor (Pa), $\bar{\bar{\tau}}_{eff}$ – effective stress tensor (Pa), k_{eff} – effective thermal conductivity (W/m·K), I – unit tensor, μ – viscosity (kg/m·s), D_i – diffusion coefficient of the tracer (m^2/s), ρ – density (kg/m^3), ρ_0– initial density (kg/m^3), u – velocity of the steel flow (m/s), t – time (s), E – energy (J), g – gravitational acceleration (m/s^2), p – pressure (Pa), T – temperature (K), h – enthalpy (J), Jj – diffusion flux (kg/m^2·s), T_0– initial temperature (K).

In non-isothermal computation, polynomial density model was employed, which is described by equation 6. For the non-isothermal conditions of steel flow through the tundish, the magnitudes of heat fluxes on particular tundish walls and bottom have been determined to be –2600 W/m^2, whereas on the regulator walls –1750 W/m^2. The losses on the free metal table surface are –15000 W/m^2 [16-24]. The wall condition with zero tangential stress was assumed on the free steel table surface. User defined scalar (UDS) transport equation were used to calculation the motion of the tracer in the liquid steel. For the description of the turbulence of steel flow through the tundish, the k-ε turbulence model was adopted, whose semi-empirical constants take on the following values: C_1 = 1.44, C_2 =1.92, σ_k =1.0, σ_ε = 1.3 [25].

Physical quantities of liquid steel as follows: viscosity 0.007 kg/m·s, heat capacity of steel 750 J/kg·K, thermal conductivity of steel 41 W/m·K, coefficient of steel thermal expansion 0.0001 1/K. At the inlet tundish, liquid steel inflow of 1.316 m/s was assumed with turbulence kinetic energy 0.0173 m^2/s^2 and energy of dissipation rate of kinetic energy 0.065137 m^2/s^3. The initial liquid steel velocity corresponded to the sequence of continuous casting of 1.5×0.225 m concast slabs at a speed of 0.9 m/min. The initial liquid steel temperature in the computer simulation was 1823 K.

The system of equations forming the mathematical model of steel flow was solved by the method of control volumes by employing discretization of the second order upwind using the sequential solver. The Semi-Implicit Method for Pressure-Linked Equations-Consistent (SIMPLEC) algorithm was used for the description of the coupling of the pressure and velocity fields in the model being solved. The controlled level of residues was at a level of at least 10^{-3}. The condition to comply with the impassable y^+ parameter values (30÷60) indicating the correct choice of the grid in the wall boundary layers was also respected.

The magnitudes of variation in the concentration of tracer in the liquid steel (numerical simulation), obtained from laboratory experiments, are represented in a dimensionless form using the equation presented by Sahai and Emi [26].

In order to explain the phenomena occurring in the tundish working space, the buoyancy number (Bu), as described by Equation 8, has been calculated.

$$Bu = \frac{g\beta\Delta T L}{u^2} \tag{8}$$

where: β – coefficient of thermal expansion (1/K), L – depth of liquid steel (m), ΔT – difference between liquid steel temperature flowed to tundish and liquid steel temperature flowed to mould (K).

The Bu number describes the effect of natural convection of modifying the fluid flow pattern, and expresses the ratio of buoyancy forces to inertial forces occurring in the system. A Bu number value above 5 means that the liquid metal flowing through the tundish will be affected by natural convection, whereas a Bu number value <1 will indicate the influence of forced convection on the steel motion.

4. Casting speed

In the continuous steel casting process, slabs are cast at varying speeds. The greater the mould thickness and width, as a rule, the lower casting speeds. Obviously, within individual groups of castings, the adjustment of casting speed is possible. The selection of casting speed is chiefly determined by chemical composition of the steel to be cast. Therefore, the casting speed must be correlated with the cooling zones (primary and secondary) so that the achieved "metallurgical length" of the CSC machine assure castings with a fully solid structure to be obtained in the cutting area. The largest changes in casting speed occur in the CSC process at its very beginning, when the casting sequence starts, whereas during the course of the process itself, changes in casting speed do not exceed, on average, 10% of the casting speed normally used for the selected steel grade. However, casting of different steel grades on the same CSC machine provides grounds for the analysis of the influence of casting speed on the hydrodynamic conditions occurring in the tundish. In this section, five casting speeds, namely 0.3, 0.6, 0.9, 1.2 and 1.5 m/min., have been examined. Liquid steel velocity at the tundish inlet for the casting variants with 0.3, 0.6, 0.9, 1.2 and 1.5 m/min. was, respectively: 0.439, 0.877, 1.316, 1.755 and 2.194 m/s. The kinetic energy of liquid steel at tundish inlet for the casting variants with 0.3, 0.6, 0.9, 1.2 and 1.5 m/min. was, respectively: 0.0019, 0.0077, 0.0173, 0.0308 and 0.0481 m^2/s^2. Casting of 1.5×0.225 m slabs was simulated, which are normally cast at a speed of 0.9 or 1 m/min. in industrial conditions. Therefore, the employed casting speeds assured the complete picture of the influence of the above-mentioned parameter on the formation of the steel flow pattern in the tundish to be obtained. The facility under examination was a tundish with a low dam. Figure 2 shows vectors fields of the flow and temperature of liquid steel. From the obtained results it can be seen that the variation in casting speed influences the liquid steel temperature field. The lower the casting speeds, the larger the difference between the temperatures of the steel flowing to the tundish

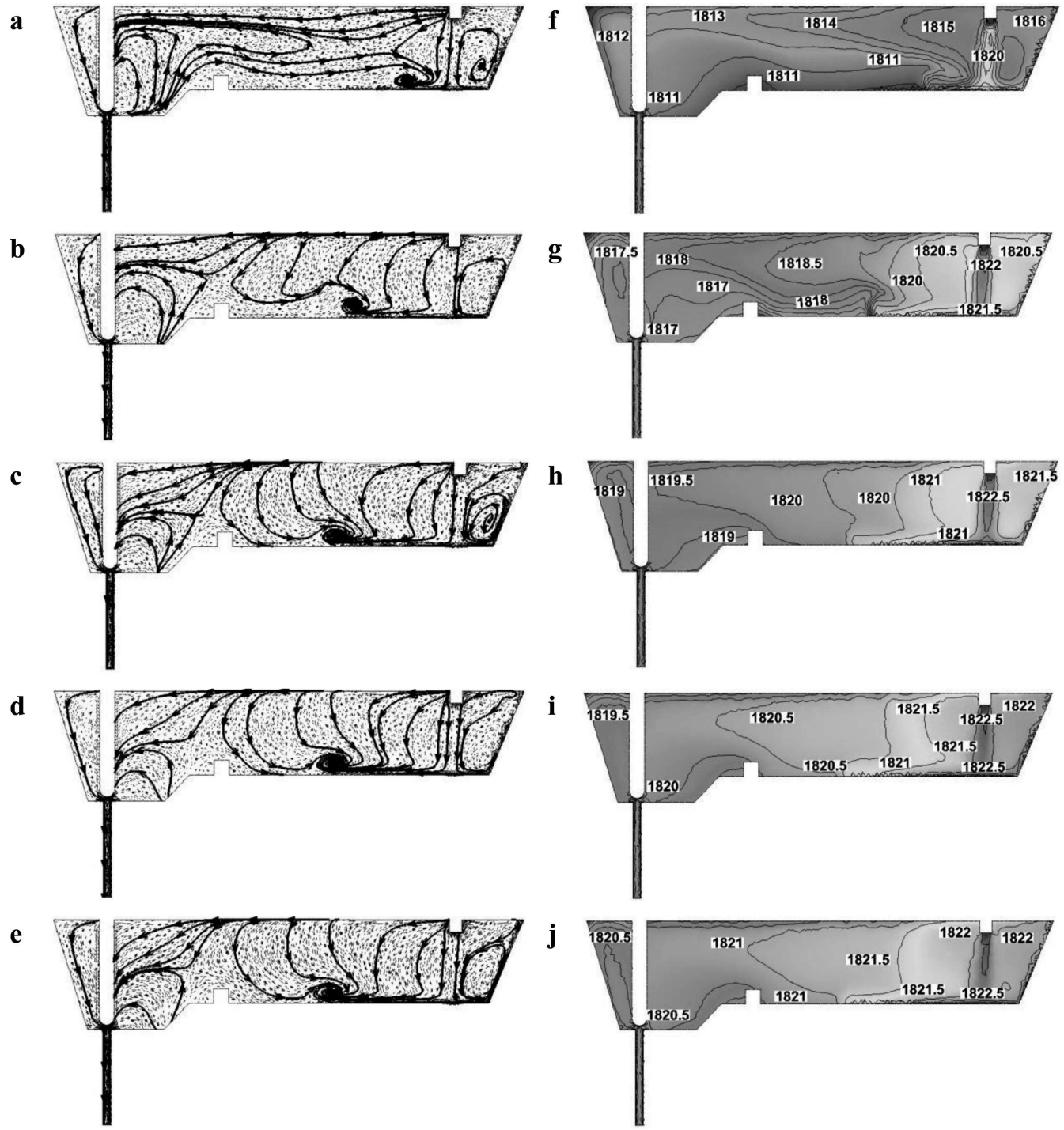

Fig. 2. Direction of liquid steel flow and temperature on the central plane: a) steel flow – casting speed 0.3 m/min, b) steel flow – casting speed 0.6 m/min, c) steel flow – casting speed 0.9 m/min, d) steel flow – casting speed 1.2 m/min, e) steel flow – casting speed 1.5 m/min, f) steel temperature – casting speed 0.3 m/min, g) steel temperature – casting speed 0.6 m/min, h) steel temperature – casting speed 0.9 m/min, i) steel temperature – casting speed 1.2 m/min, j) steel temperature – casting speed 1.5 m/min

and the steel flowing to the mould. In all simulation variants, the temperature of the liquid steel flowing to the tundish was 1823 K. For the casting speed of 0.3 m/min., the temperature gradient between the pouring zone and the stopper system zone in the central tundish part amounted to 12 K. Whereas, in the case of casting at the nominal casting speed or higher speeds, the temperature gradient was contained in the range from 4 to 2.5 K. Therefore, the longer the residence of steel in the tundish, the more intensive its cooling due to the removal of heat through the tundish walls and bottom and the free steel table surface. The average time of liquid steel residence in the tundish for the casting variants with 0.3, 0.6, 0.9, 1.2 and 1.5 m/min. was, respectively: 1941, 970, 646, 484 and 387 seconds. The change in liquid steel temperature affects the liquid steel flow pattern. Intensive cooling of the liquid steel in the tundish at the casting speed of 0.3 m/min. translates into an increase in the density of the steel and its flow in the tundish. A clear stratification between the warmer

stream feeding the tundish and the cold reverse stream flowing from the stopper system towards the pouring zone can be seen (Figs. 2a and 2f). As the steel temperature gradient decreases due to the increase in the casting speed, the stabilization of the flow pattern in the central tundish part is observed, which is distinguished by the liquid steel stream clearly descending towards the bottom and the steel circulation region situated in the mid-distance between the low dam and the pouring zone. The steel circulation, observed in the lower part of the tundish, changes its position with decreasing casting speed. The lower the casting speed, the closer to the feed zone the circulation region is. As it is produced by the collision of the feed stream with the reverse stream flowing from the stopper zone, this evidences the domination of the reverse stream in the creation of the flow pattern in the lower part of the tundish working space. For a fuller understanding of the reasons for which the pattern of flow in the tundish varies with the change in the casting speed, the values of the buoyancy number (Bu) have been calculated for the casting variants under analysis. Table 1 presents results for the Bu number in two tundish regions, i.e. from the decline zone to the feed zone, where the steel level is 0.7 m, and in the stopper rod system zone, where the bottom is lowered by 0.2 m. The data in Table 1 suggests that the increase in casting speed translates into the average speed of liquid steel in the tundish working volume. In addition, with the decrease in casting speed, the difference between the temperature of steel feeding the tundish and the temperature of steel supplying the mould increases. Both the liquid steel flow velocity and the temperature gradients influence heavily the Bu number value. Thus, reducing the casting speed below the standard casting speed of 0.9 m/min. results in an increase in the Bu number value and the domination of forces associated with natural convection in the flow pattern forming process. Above the standard casting speed, only inertial motion-related forces create the flow pattern. For the tundish, the stimulus that forces the specific behaviour of the fluid (liquid steel) is the feed stream flowing to the tundish. The next research step in the analysis of the flow pattern forming in different casting conditions was to record the E and F-type RTD characteristics and to describe the pattern of flow. Figure 3 represents the distribution of tracer concentration as a function of time for the examined casting speeds. The RTD characteristics shown in Figure 3 confirm the fact observed in the analysis of the vector fields of liquid steel flow and temperature that a definite change in the hydrodynamic pattern in the tundish working space occurs at the point of the casting speed slowing down to a value of 0.3 m/min. This situation is reflected in the increase in continuous casting length corresponding to the transient zone and the increase in the share of stagnant volume flow in the tundish during casting at a casting speed of 0.3 m/min (Table 2).

TABLE 1

Dimensionless Bu number for consider variants of casting speed

Casting speed, m/min	Average velocity of steel, m/s	Temperature difference ΔT, K	Steel level, m	Bu number, –
0.3	0.0165	13	0.7	32.8
			0.92	43.1
0.6	0.0253	7	0.7	7.5
			0.92	9.9
0.9	0.0357	5	0.7	2.7
			0.92	3.5
1.2	0.0471	4	0.7	1.2
			0.92	1.6
1.5	0.0595	3	0.7	0.6
			0.92	0.8

TABLE 2

Transition zone and flow structure for different casting speed

Casting speed, m/min	Transition zone		Flow structure		
	Time, s	Length of slab, m	Stagnant flow, %	Plug flow, %	Ideal mixing flow, %
0.3	2637	13.18	40.1	12.8	47.1
0.6	1151	11.51	33.5	9.5	57
0.9	764	11.46	32.1	10.4	57.5
1.2	579	11.58	32.8	9.8	57.4
1.5	464	11.60	32.7	10.1	57.2

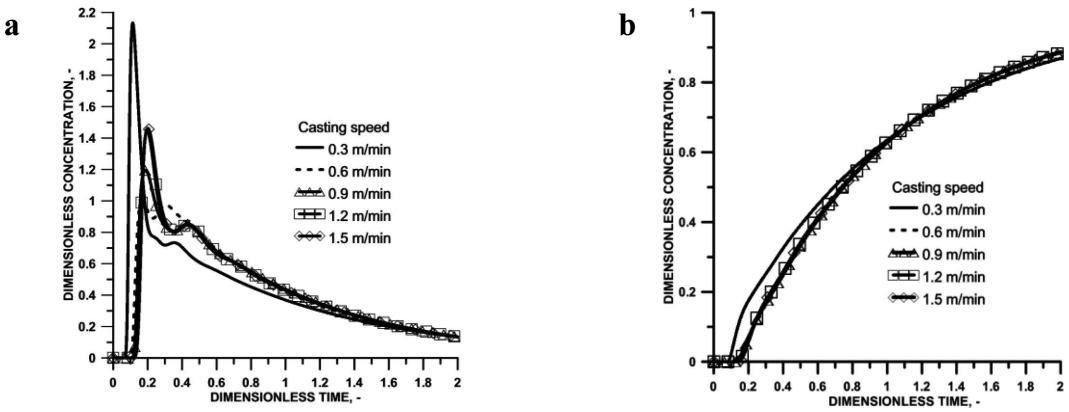

Fig. 3. RTD characteristic for consider variants of casting speed: a) RTD type E, b) RTD type F

5. Thermal condition

In the continuous steel casting process, the liquid steel temperature varies most intensively in the primary cooling zone (the mould) and in the secondary cooling zone (the tensioning-bending-straightening roller segments). In the above-mentioned zones, the differences in temperature between the liquid steel and the solidifying steel reach a level of several dozen degrees Celsius. Whereas, in the tundish, stable thermal conditions should be provided in order to maintain the required casting temperature within the whole melt casting period. The complete thermal stabilization and homogenization of liquid steel in the tundish is not, however, possible due to the constant cooling of the steel by contacting the tundish walls and bottom and the tundish powder being spread over the steel table. For this reason, refractory materials used for construction of the tundish working space and insulating powders should reduce the magnitude of the heat flux from the steel to the environment. In view of the fact that tundishes are being equipped with various flow control devices and the process of creating specific hydrodynamic conditions is influenced also by the temperature gradient, computer simulations of liquid steel flow under isothermal and non-isothermal conditions were performed. Hydrodynamic conditions were examined in three tundish furniture variants, i.e. the tundish with a low dam, the tundish with a high dam and the tundish with STC. Figure 4 shows maps of liquid steel flow through the central part of the tundish. In the tundish with the low dam, the vector field of flow, both in isothermal and non-isothermal conditions, is characterized by a very similar pattern of distribution of individual steel streams. Between the stopper rod system zone and the metal pouring zone the liquid steel flows towards the tundish bottom. In both simulations, similar liquid steel circulation regions also occur, namely at the bottom and in the pouring zone of the tundish (Fig.4a and 4d). First differences that occur in the flow pattern are visible in the high dam tundish (Figs. 4b and 4e). In isothermal conditions, a liquid steel circulation region forms between the high and low dams, which disappears in non-isothermal conditions, being replaced by a reverse stream flowing from the stopper rod system zone to the high dam. The largest difference in flow pattern is visible for the tundish with STC, because a large metal circulation region can be seen between the turbulence controller and the low dam in the isothermal simulation, which is fed by the reverse stream flowing from the stopper rod system zone (Fig. 4c). By contrast, in the non-isothermal simulation, part of the reverse stream flows towards the stopper rod, while the part that is directed towards the pouring zone flows around the circulation zone and then, immediately under the liquid steel table, flows back towards the stopper rod system (Fig. 4f). The recorded differences in hydrodynamic patterns are related to the average velocities of liquid steel within the steel volume,

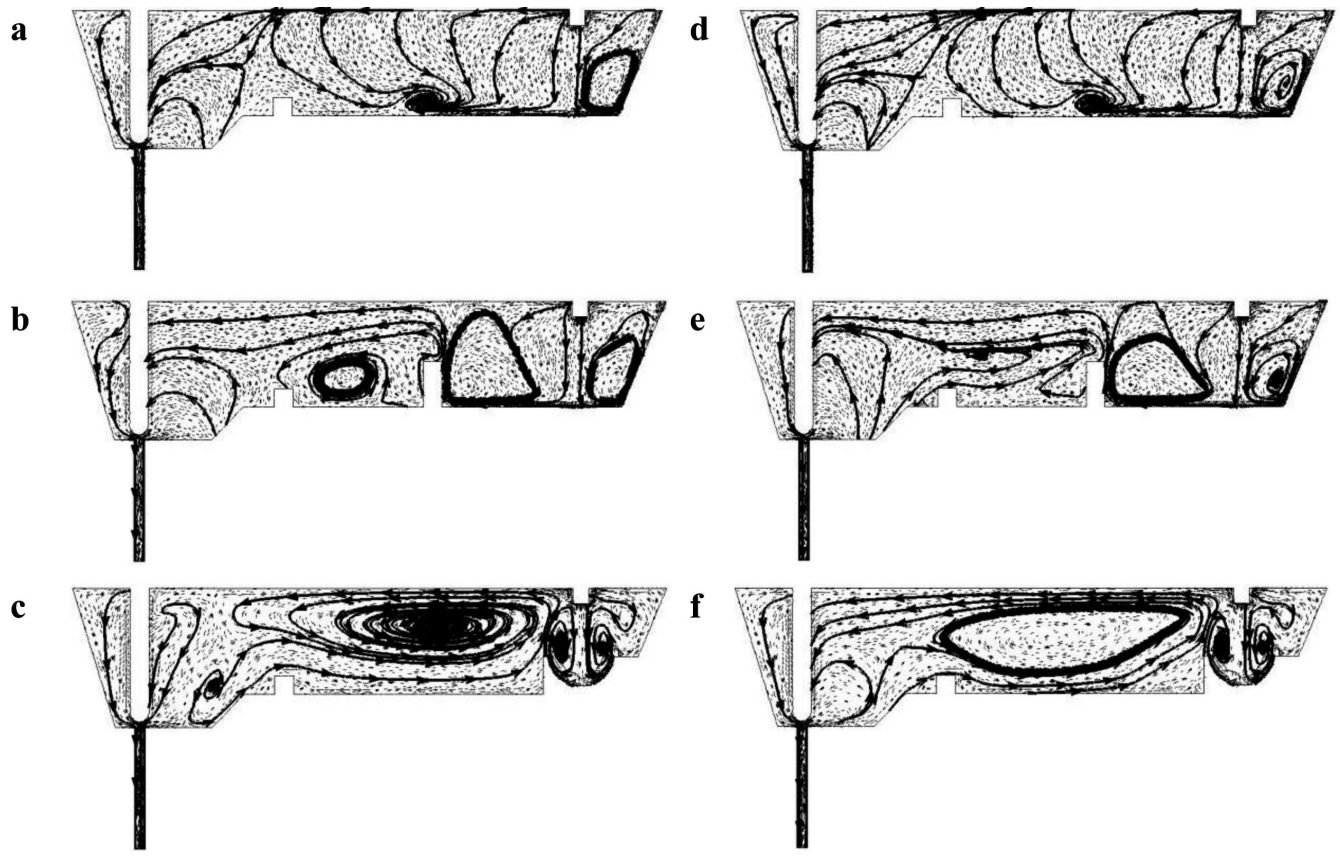

Fig. 4. Liquid steel flow on the central plane: a) direction of liquid steel flow in the tundish with low dam – isothermal condition, b) direction of liquid steel flow in the tundish with high dam – isothermal condition, c) direction of liquid steel flow in the tundish with STC – isothermal condition, d) direction of liquid steel flow in the tundish with low dam – nonisothermal condition, e) direction of liquid steel flow in the tundish with high dam – nonisothermal condition, f) direction of liquid steel flow in the tundish with STC – nonisothermal condition

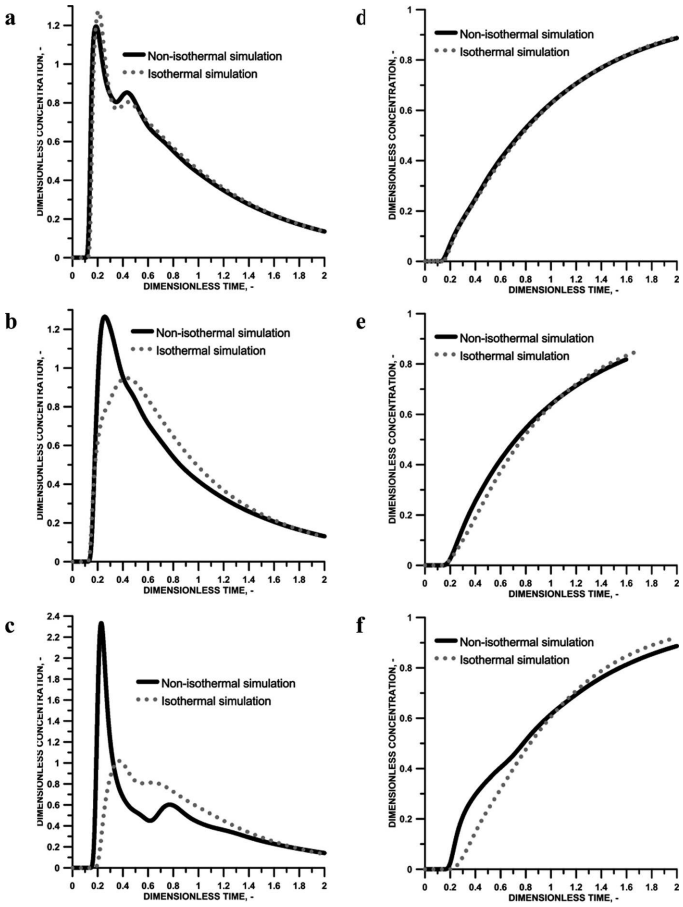

Fig. 5. RTD characteristic: a) RTD type E – tundish with low dam, b) RTD type E – tundish with high dam, c) RTD type E – tundish with STC, d) RTD type F – tundish with low dam, e) RTD type F – tundish with high dam, f) RTD type F – tundish with STC

as well as to the occurring metal temperature gradient. In the isothermal simulations, the average velocity of liquid steel flow was 0.034, 0.031 and 0.020 m/s, respectively, in the tundish with the low-dam, the high dam and STC. The lowest speed recorded in the tundish with STC results from the fact that this device belongs to the group of devices limiting the force of momentum of liquid steel flowing into the tundish. Therefore, if the tundish furniture affects the velocity of steel flow in the tundish working part, then under non-isothermal conditions, with a likely occurrence of a temperature gradient, natural convection forces might influence the flow pattern. In view of the above, the values of the Bu number were calculated, and the results are summarized in Table 3. Reducing the liquid steel flow velocity results in an increase in the Bu number and the influence of natural convection forces on the creation of steel stream flow conditions. In all of the considered non-isothermal simulations, the temperature gradient between the ladle shroud gate and tundish nozzle amounted to 5K; in some locations, however, it is larger. This reflects in localized differences in flow pattern, which are visible on the vector maps. Moreover, the performed simulations indicate that, for constant, specific thermal conditions, the FCD (flow control device) will have the effect of modifying the liquid steel motion. The observed differences are most clearly demonstrated by the E and F-type RTD characteristics represented in Figure 5. For the low-dam tundish, the differences in the shape of the curves for the considered thermal conditions are very small (Figs. 5a and 5d). By contrast, in the high-dam tundish variant, a shift of the curve peak towards the axis of ordinates can be seen, which is reflected in the worsening of the hydrodynamic conditions (Figs. 5b and 5e). The largest difference occurs in the hydrodynamic pattern recorded in the tundish with STC (Figs. 5c and 5f). The definitely higher value of tracer concentration in the peak (in the non-isothermal simulation) suggests an increase in stagnant volume flow. The observed transformation of the RTD curves signalling changes in the flow pattern has been confirmed by the calculated values of the transient zone extent and the flow pattern. For the considered variants of the tundish with the low dam, the high dam and STC, the differences in the length of continuous casting transient zone between the isothermal and non-isothermal simulations were, respectively: 0.14, 1.13 and 2.59 m. The increase in continuous casting transient zone length was caused directly by the worsening of hydrodynamic conditions in the non-isothermal conditions by the increase in the share of stagnant volume flow. The greatest increase in the stagnant volume flow zone was recorded in the tundish with STC, which amounted to 11.2%.

TABLE 3
Dimensionless Bu number for consider variants of tundish equipment – nonisothermal simulation

Type of flow control devices	Average velocity of steel, m/s	Temperature difference ΔT, K	Steel level, m	Bu number, –
low dam	0.0357	5	0.7	2.7
			0.92	3.5
high dam	0.033	5	0.7	3.2
			0.92	4.1
STC	0.024	5	0.7	6
			0.92	7.8

TABLE 4
Transition zone and flow structure for isothermal and nonisothermal condition

Type of flow control devices	Type of thermal condition	Transition zone		Flow structure		
		Time, s	Lenght of slab, m	Stagnant flow, %	Plug flow, %	Ideal mixing flow, %
low dam	isothermal	754	11.32	31	12.1	56.9
	nonisothermal	764	11.46	32.1	10.4	57.5
high dam	isothermal	657	9.86	28.2	24	47.8
	nonisothermal	733	10.99	33.1	15	51.9
STC	isothermal	619	9.28	21	21.4	57.6
	nonisothermal	791	11.87	32.2	14.2	53.6

6. Summary

From the performed computer simulations it can be found that:

- During casting of slabs at a constant casting speed (±10% of the nominal speed) the hydrodynamic pattern in the tundish will not change significantly;
- The modification of the pattern of flow in the tundish is only effected by changing the casting speed to below the nominal casting speed value;
- With a decrease in the velocity of liquid steel flowing through the tundish the share of natural convection forces in the creation of hydrodynamic conditions in the working space of the facility under examination increases;
- The increase in casting speed causes the tundish feed stream to obtain a driving force necessary for the creation of hydrodynamic conditions within the entire liquid steel volume;
- Simulation of the real conditions of steel flow through the tundish, while not considering the non-isothermal conditions, will distort the description of the hydrodynamic state of the facility under examination;
- The hydrodynamic flow pattern is affected by the type of employed flow control device which directly influences the average velocity and distribution of temperature of liquid steel in the working space of the tundish.

Acknowledgements

The research work has been financed from the budget resources allocated to research in the years 2012-2013 in the framework of the IuventusPlus programme.

REFERENCES

[1] I. Staniewski, W. Derda, Archiv. of Metall. and Mater. **50**, 843-856 (2005).
[2] T. Telejko, Z. Malinowski, M. Rywotycki, Archiv. of Metall. and Mater. **54**, 837-844 (2009).
[3] H. Kania, J. Gawor, Archiv. of Metall. and Mater. **57**, 339-345 (2012).
[4] A. Sorek, Z. Kudliński, Archiv. of Metall. and Mater. **57**, 371-377 (2012).
[5] A. Burbelko, J. Falkus, W. Wypartowicz, K. Sołek, P. Drożdż, M. Wróbel, Archiv. of Metall. and Mater. **57**, 379-384 (2012).
[6] M. Rywotycki, K. Miłkowska-Piszczek, L. Trębacz, Archiv. of Metall. and Mater. **57**, 385-393 (2012).
[7] A. Cwudziński, Ironmaking Steelmaking **37**, 169-180 (2010).
[8] L. Bulkowski, U. Galisz, H. Kania, Z. Kudliński, J. Pieprzyca, J. Barański, Archiv. of Metall. and Mater. **57**, 363-369 (2012).
[9] A. Cwudziński, and J. Jowsa, Archiv. of Metall. and Mater. **53**, 749-761 (2008).
[10] X.-M. Yang, S.-X. Liu, J.-S. Jiao, M. Zhang, J.-P. Duan, L. Li, and C.-Z. Liu, Steel Res. **83**, 269-287 (2012).
[11] V. Singh, S.K. Ajmani, A.R. Pal, S.K. Singh, and M.B. Denys, Ironmaking Steelmaking **39**, 171-179 (2012).
[12] K. Chattopadhyay, M. Isac, and R.I.L. Guthrie, Ironmaking Steelmaking **39**, 454-462.
[13] S. Sarkar, R. Sambasivam, S.K. Ajmani, and M.B. Denys, Ironmaking Steelmaking **39**, 540-549 (2012).
[14] J. Palafox-Ramos, J. De J. Barreto, S. López-Ramirez, R.D. Morales, Ironmaking Steelmaking **28**, 101-109.
[15] T. Merder, Metalurgija **52**, 161-164 (2013).
[16] S. Chakraborty, and Y. Sahai, Metall. Mater. Trans. B **23B**, 153-167 (1992).
[17] R.D. Morales, S. Lopez-Ramirez, J. Palafox-Ramos, and D. Zacharias, ISIJ Int. **39**, 455-462 (1999).
[18] Y. Miki, and B.G. Thomas, Metall. Mater. Trans. B **30B**, 639-654 (1999).
[19] M.A. Barron-Meza, J. De J. Barreto-Sandoval, and R.D. Morales, Metall. Mater. Trans. B **31B**, 63-74 (2000).
[20] S. Lopez-Ramirez, J. De J. Barreto, J. Palafox-Ramos, R.D. Morales, and D. Zacharias, Metall. Mater. Trans. B **32B**, 615-627 (2001).
[21] R.D. Morales, S. Lopez-Ramirez, J. Palafox-Ramos, and D. Zacharias, Ironmaking Steelmaking **28**, 33-43 (2001).
[22] R.K. Singh, A. Paul, and K. Ray, Scand. J. Metall. **32**, 137-146 (2003).
[23] S. Lopez-Ramirez, J. De J. Barreto, P. Vite-Martinez, J.A. Romero Serrano and C. Duran-Valencia, Metall. Mater. Trans. B **35B**, 957-966 (2004).
[24] L. Zhang, Steel Res. **76**, 784-796 (2005).
[25] O.J. Ilegbusi, M. Iguchi, W. Wahnsiedler, Mathematical and physical modeling of materials processing operations, Boca Raton, Chapman & Hall/CRC 2000.
[26] Y. Sahai, and T. Emi, Tundish technology for clean steel production, Singapore, World Scientific Publishing Co. Pte. Ltd 2008.

Received: 20 August 2013.